

MICROWAVE INTERFEROMETERS FOR NON-CONTACT VIBRATION MEASUREMENTS ON LARGE STRUCTURES

by

Charles R. Farrar, Timothy W. Darling, Albert Migliori, and William E. Baker

Los Alamos National Laboratory

ABSTRACT

This paper describes a non-contact vibration measuring system that is based on a microwave interferometer similar to those used to detect the presence of people in monitored areas. Displacement response of a target surface on the structure relative to the interferometer is measured by analyzing the interference in microwaves reflected off the vibrating target surface. The system was built from commercially available off-the-shelf electronic components and, unlike most commercially available far-field non-contact vibration sensors, it does not require a mounted target when used to measure the response of metallic and concrete structures. In this study the interferometers are coupled with homodyne detection hardware and software to make low-noise measurements during swept-sine tests. These interferometers can also be used to detect static displacements and the transient response of the structure. In addition to its non-contact feature, this system offers other advantages including low cost, quick setup time, a wide frequency range of response, and portability. An application of these sensors to the measurement of vibration response on a bridge structure in a non-contact manner is summarized. Resonant frequencies of the bridge that were identified with the microwave interferometers are compared to similar quantities measured with conventional accelerometers. In all cases, resonant frequencies identified from data obtained with the microwave interferometers were within 2.2 percent of the resonant frequencies determined from data obtained with the conventional accelerometers.

I. Introduction

The primary types of sensors used for vibration testing are piezoelectric or piezoresistive seismic accelerometers. For experimental modal analysis applications piezoelectric accelerometers are most commonly used. They have adequate signal-to-noise ratio, bandwidth, and are usually small enough relative to the structure being tested so as not to alter the structure's dynamic properties. Piezoelectric accelerometers are relatively inexpensive (typically in the range of 250-1000 Dollars US, 1997) and accurate. However, there are problems associated with these devices particularly when they are applied to the vibration testing of very large structures, when they are used in hazardous environments, and when the mass of the accelerometer is significant relative to the mass of the structure being tested. Although mode shape and operating shapes of a structure are routinely measured with conventional accelerometers, these sensors do not provide a direct measurement of displacement, which is often of interest for the study of a structure's operating vibration shapes (the superposition of many mode shapes).

Accelerometers must be mounted at the appropriate locations that are representative of the structure's motion, and access may be a problem, particularly if the tests are being performed in hazardous environments such as radiation or high voltage areas. Also, use of these transducers requires hardwiring from the transducer to the data acquisition system. When the structure is

large, the effort associated with mounting and wiring the accelerometers is typically the most time-consuming task associated with the test, and can subject the test crew to hazardous conditions. As an example, the mounting and wiring of 26 accelerometers on a 130 m (425 ft) segment of the bridge discussed in this paper required approximately 30 person-days (much of this time was spent on narrow catwalks 6.1 - 12 m (20 - 40 ft) above the ground), while an actual test took only 2-3 hours.

Another problem associated with piezoelectric accelerometers is their lower and upper frequency limits. For the accelerometer being used, one must ensure that its bandwidth is adequate for the response of the structure being studied. This consideration necessitates a large stock of accelerometers to cover the many types and sizes of structures which may be studied. For large structures, low modal frequencies are encountered, and they may be at or below the low frequency cut-off of many accelerometers. Also, even though large structures generally have low modal frequencies, impact loading from ambient sources (such as observed when trucks hit expansion joints in bridges) can have high frequency components thus causing the accelerometers to respond at high frequencies. At these high frequencies the accelerometer may resonate which can lead to inaccurate measurements. A detailed summary of such a problem can be found in [1].

There are non-contact, near-field and far-field displacement transducers that are commercially available. The near-field non-contact transducers include feedback-type capacitive devices, eddy-current transducers, mutual inductance devices, variable reluctance devices, and fiber-optic sensors [2,3]. Because of the need for a fixed reference location to mount the near-field non-contact sensors, these devices do not offer any significant advantage over conventional accelerometers when testing large structures or structures in hazardous environments and, hence, will not be discussed further. Laser based systems are primarily used for far-field non-contact motion sensors. The principles of operation for these far-field transducers fall into one of three categories: 1.) linear encoders for motion transverse to the laser beam, 2.) optical interference for motion in the direction of the laser beam, or 3.) the laser Doppler effect, again for motion in the direction of the laser beam. The encoders and the interferometers generally use some type of fringe counters to obtain a displacement reading. Some encoders also employ gratings to measure displacement. The laser Doppler unit is based upon the well known Doppler shift of frequency, but for a laser light frequency rather than an audio frequency. Generally, these commercial units meet the measurement specifications needed for the vibration analysis application, but they also have drawbacks. First, each type requires the mounting of a special reflector at the point of interest, and second, they are, in general, too expensive for multiple channel applications making mode shape measurement impractical. Scanning laser vibrometers can alleviate this problem. However, the scan area of these devices limits them to measuring relatively small areas of a large structure.

This paper will describe a non-contact vibration sensor that overcomes some of the problems associated with other types of commercially available far-field non-contact vibration measurement devices. The sensor is based on a microwave interferometer that has been previously developed to detect the motion of people in monitored areas [4]. Application of these sensors to vibration monitoring of a bridge and comparisons of modal properties identified by these sensors with comparable quantities obtained from standard piezoelectric accelerometer measurements are presented.

II. Sensor Description

The microwave interferometer consists of an aluminum parabolic dish, with an X or K band microwave source/receiver horn mounted at the focus. The microwave source is similar to that used for intruder alarms and automated door openers and, hence, it posed no safety hazard to people. The horn may have a commercial Gunn diode transceiver unit ("Gunnplexer") attached to it, or it may be connected by a wave guide to other microwave source and receiver components. When power is applied to the Gunn diode, or other microwave source, it oscillates at microwave frequencies and transmits an electromagnetic wave through a wave guide, then off the parabolic dish to the object whose motion is to be measured. The wavelengths of the microwave (1.25 cm – 3.00 cm) are long enough to pass through potential interfering sources such as airborne dust, but are short enough that it will reflect off larger objects. The optical axis of the sensor is aligned so that it is approximately perpendicular to the target surface. A portion of the microwave source forms a reference signal that is transmitted to a mixer diode. Microwaves, reflected from the target surface, are focused by the dish back into the transceiver and mixer diode where they interfere with the reference signal waves and form a standing wave pattern. The amplitude of the standing wave will depend upon the phase shift between the reference signal and the signal reflected off the target surface. The phase shift is, in turn, dependent on the distance of the target surface from microwave source, up to a complete wavelength shift. When the target surface moves perpendicular to the microwave, the signal across the mixer diode changes as the distance of the target surface from the interferometer changes. Finally, the signal from the mixer diode is amplified and fed into an analog-to-digital converter where the voltage-time history can be converted, with an appropriate calibration factor, to a digital displacement-time history. This measurement method is analogous to optical interferometry. To account for various sources of phase shifts other than those caused by the motion of the target surface, adjustments were made to the phase of the pattern by changing the frequency of the source a small amount. The sources include phase shifts caused by changes in dead loads on the bridge and phase shifts caused by thermal effects on the Gunn Oscillator. This change was accomplished by putting a tuning voltage on a variable capacitance (varactor) diode that is located in the microwave transmitter assembly. Figure 1 shows a schematic of the microwave interferometer, and Fig. 2 shows the actual sensor supported by a drum under the plate girder whose displacement was being monitored. For the application shown in Fig. 2 the target surface was the bottom flange of a plate girder. This flange had a width approximately equal to the diameter of the parabolic dish.

One primary advantage of this system over commercially available far-field non-contact vibration measuring devices is that for common construction materials the microwave interferometer does not require a target to be mounted on the monitored surface. This feature is advantageous when working in hazardous environments and when access to the target surface is difficult. The sensor has been tested on metallic surfaces and concrete, both of which have shown adequate reflectivity.

The focused area of the microwave will be approximately equal to the size of the parabolic dish. Therefore, the displacement being measured is an average of the target surface over an area

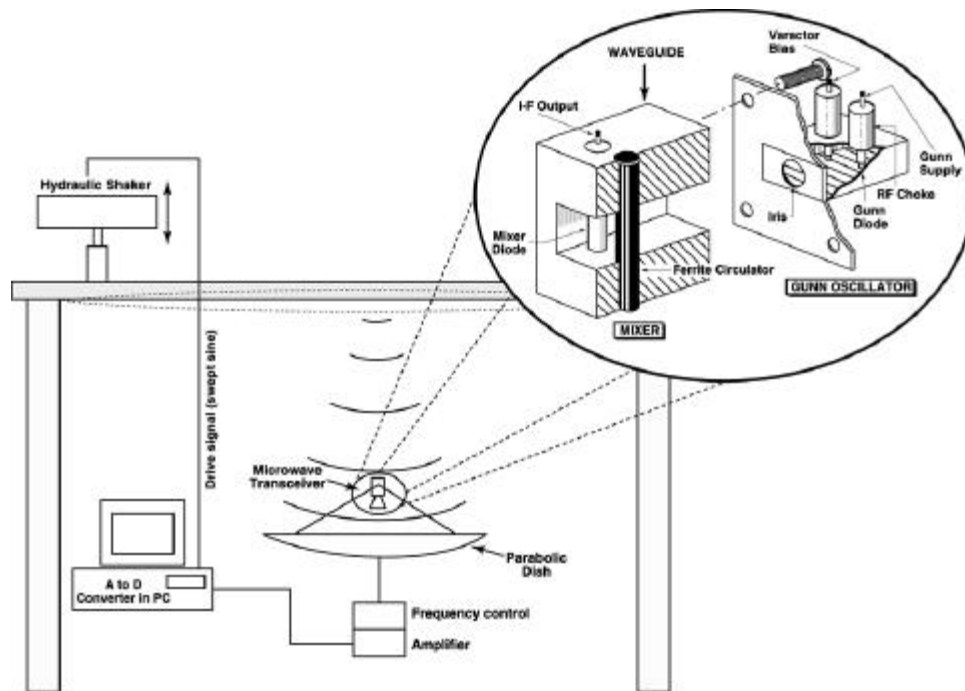


Figure 1

ESA-EA
CFM-1

Fig. 1 Schematic diagram of the microwave interferometer.



Fig. 2. The microwave interferometer setup in the field to measure the response of a plate girder.

approximately equal to the size of the dish. Although not fully quantified at this time, diffraction of the microwaves will cause this area to increase with distance from the dish. Decreasing the size of dish will increase the diffraction. Objects that are moving in close proximity to the surface being monitored can cause spurious readings. The sensors have a theoretical range on the order of several hundred meters with the limiting factor being the reflectivity of the surface being monitored. In practice the sensor has been used at distances of up to 65 m (210 ft) from the target. Ideally the surface to be monitored should be flat and perpendicular to the microwave beam, however, reflection will occur from curved surfaces. The curvature will reduce the strength of the reflected signal, but for the applications investigated to date it does not influence the ability to measure an average translation of the surface over the target area. In theory, with the proper calibration changes in the reduction of the signal strength can be correlated to changes in curvature of the surface. Further investigations are needed to evaluating the accuracy of the sensors when monitoring the response of curved surfaces and surfaces exhibiting small rotations.

Resolutions on the order of 0.1 mm (0.004 in.) have been obtained to date for responses at frequencies less than 10 Hz. The wavelengths of the microwaves are the limiting parameter with regard to resolution. Peak amplitudes that could be accurately measured were originally limited to one-quarter of the microwave's wavelength, or 6.1 mm (0.24 in.). When data acquisition hardware and software were coupled with the sensor such that the system could act in a fringe-following mode, amplitudes of 7.0 cm (2.75 in.) have been accurately measured at a distance of approximately 4.9 m (16 ft.). In the fringe-following mode phase shifts between the reference signal and the reflected signal greater than 360 degrees can be measured by standard technique employed in optical interferometry. Frequency responses in the range of DC to 17 kHz have been measured in a laboratory using a loud speaker as the vibrating target. Although not yet quantified, it is anticipated that the upper frequency range of the system will be limited by the feed-back time of the fringe follower.

III. Data Acquisition

The microwave interferometer can be used to study transient vibration signals by digitizing the voltage-time history emitted from the amplifier and analyzing the signal with standard signal processing software packages. In practice, the microwave interferometers were used to acquire vibration data in a low frequency homodyne detection mode. Figure 3 shows a schematic diagram of the hardware and software that has been coupled with the interferometer for both random signal analysis and the homodyne detection mode.

When used in the homodyne detection mode, a dual programmable signal generator provided a sine wave source at a given frequency, ω , to an amplifier, which is used to drive a shaker. This source is designated $A\sin(\omega t)$. Vibrations are detected by the microwave interferometer as discussed above, digitized and fed into the homodyne mixer. For a linear system subjected to a harmonic excitation, the output will be at the same frequency as the input, but with different amplitude and phase. The output signal from the interferometer is designated $B\sin(\omega t + \phi)$. The same signal that was used to drive the shaker was also fed into the mixer along with a similar signal shifted 90 degrees in phase, which is designated $A\cos(\omega t)$. The homodyne mixer multiplies the output signal from the interferometer by the two signals, $A\sin(\omega t)$ and $A\cos(\omega t)$, yielding (after some trigonometric manipulation) two signals, $H_1(t)$ and $H_2(t)$, where

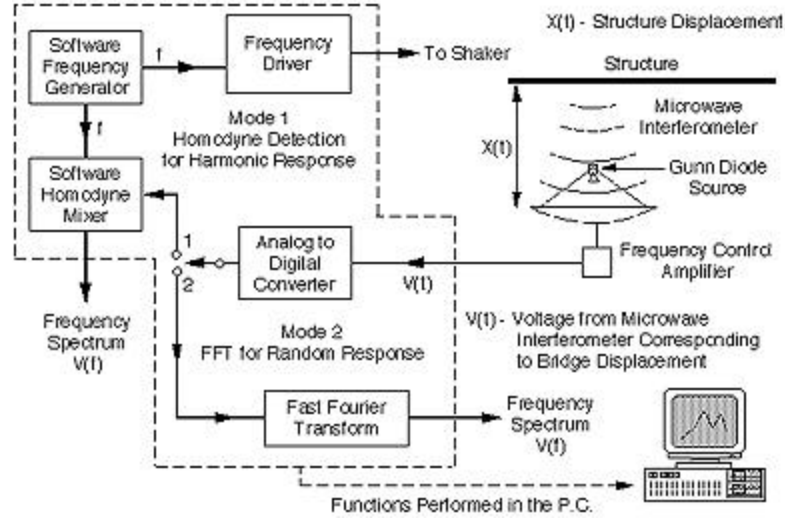


Fig. 3 Schematic diagram of the signal processing software that was coupled with the microwave interferometer.

$$H_1(t) = 0.5 AB \cos(\phi) - 0.5 AB \cos(2\omega t + \phi), \text{ and} \quad (1)$$

$$H_2(t) = 0.5 AB \sin(\phi) + 0.5 AB \sin(2\omega t + \phi), \text{ respectively.} \quad (2)$$

These signals are composed of a DC component represented by the first term in each equation, and an AC component that has a frequency of 2ω . Numerous time averages are taken causing the AC terms in Eqs. 1 and 2 to go to zero. The remaining DC components in Eqs. 1 and 2 are squared (to remove the phase angle dependence) and added, yielding

$$H_1^2(t) + H_2^2(t) = 0.25 A^2 B^2 (\cos^2(\phi) + \sin^2(\phi)) = 0.25 A^2 B^2. \quad (3)$$

Because the amplitude of the source signal, A , is known, the amplitude of the response, B , can be extracted. The computer then steps to the next frequency, recording and plotting the response amplitude values as a function of the excitation (and response) frequency. The advantage of this method over conventional modal testing, which typically uses broad-band excitation from a shaker or impulse input, is that all the excitation energy is put in at a specified frequency thus enhancing the ability to identify modes other than the predominant ones. This advantage is independent of the type of sensor being used with the homodyne detection system. The primary disadvantage of this method is the time required performing the swept-sine test.

IV. Application to a Bridge Vibration Test

Two microwave interferometers that used a Gunnplexer microwave source and a 61-cm diameter (24-in dia.) parabolic dish were used during vibration testing of the I-40 bridge over the Rio Grande in Albuquerque, NM. The I-40 bridges over the Rio Grande that were tested consisted of twin bridges, one for each traffic direction, each made up of a concrete deck supported by two welded-steel plate girders and three steel stringers. Loads from the stringers were transferred to the plate girders by floor beams located at 6.1 m (20 ft) intervals. Cross-bracing was provided between the floor beams. Each bridge was made up of three identical sections. Except for the

common pier located at the end of each section, the sections were independent. A section had three spans; the end spans were of equal length, approximately 39.9 m (131 ft), and the center span was approximately 49.7 m (163 ft) long. Five plate girders were connected with four bolted splices to form a continuous beam over the three spans. The portions of the plate girders over the piers had increased flange dimensions, compared with the mid-span portions, to resist the higher bending stresses at these locations. Figure 4 shows an elevation view of the portion of the bridge that was tested. The cross-section geometry of each bridge is shown in Fig. 5. Connections that allowed for longitudinal thermal expansion, labeled "exp" in Fig. 4 as well as a connection that prevented longitudinal translation, labeled "pinned" in Fig. 4, were located at the base of each plate girder, where the girder was supported by a concrete pier or abutment. All subsequent discussions of the bridge will refer to the bridge that carried east-bound traffic, particularly the three eastern spans, which were the only ones tested.

Forced vibration tests using a hydraulic shaker mounted on the bridge deck were first performed on the bridge in its undamaged state. A detailed description of the shaker can be found in [5]. Next, damage was introduced into one plate girder incrementally and the vibration tests were repeated. The damage that was introduced was intended to simulate cracking that has been observed in plate girder bridges. Four levels of damage were introduced to the middle span of the north plate girder close to the seat supporting the floor beam at mid-span. Damage was introduced by making various torch cuts in the web and flange of the girder. The first level of damage consisted of a 61-cm-long (24 in) cut approximately 0.95-cm-wide (0.38-in-wide) centered at mid-height of the web. Next, this cut was continued to the bottom of the web. During this cut the web, on either side of the cut, bent out of plane approximately 3 cm (1 in). The flange was then cut half way in from either side directly below the cut in the web. Finally, the flange was cut completely through leaving the top 120 cm (48 in) of the web and the top flange to carry the load at this location. The various damage levels are shown in Fig. 6.

As discussed above, a computer controlled sine wave generator provided a fixed frequency harmonic input to drive the hydraulic shaker. The amplitude of the vertical response of the plate girder's bottom flange was measured remotely by the two microwave interferometers that were located directly under the bottom flange of the north and south plate girder at the middle of the center span. For a given excitation frequency, the response amplitude at that frequency was extracted by the homodyne detection system. The computer then stepped to another frequency to repeat the measurement. The response of the bridge was measured over a frequency range of 2 to 5 Hz, in steps of 0.05 Hz with 80 s time windows measured at each frequency increment. A complete fully automated scan from 2 Hz to 5 Hz in 0.05 Hz steps took approximately 1.5 hours. The long time windows were used to average the estimates of the peak response amplitudes obtained at each frequency step. The primary source of noise in these measurements was mechanical, not electrical. Random impact-type excitations from trucks on the adjacent bridge, as they hit the expansion joints, produced broad-band inputs causing an extraneous response component at the frequency of the harmonic excitation. The homodyne detection method does not filter this extraneous response component. This noise source is not related to the microwave measurements and was a problem for the modal tests performed with conventional accelerometers as well.

The accumulated data set was then fit (by minimizing a chi-squared error term) with an analytical function to extract the resonant frequencies and modal damping associated with each resonance

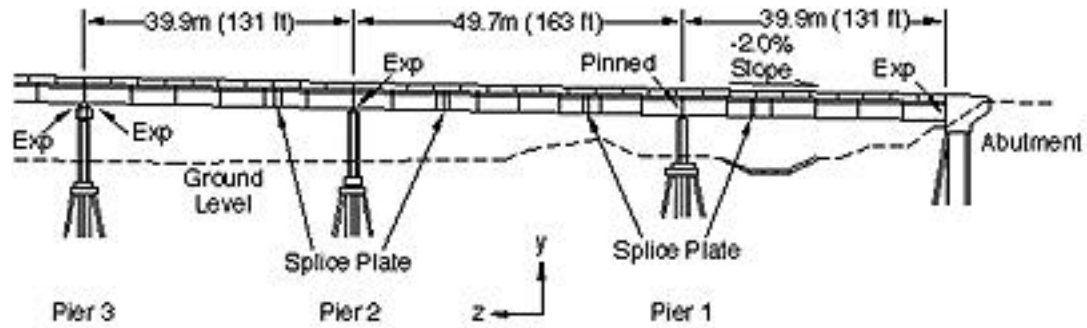


Fig. 4 Elevation view of the portion of the eastbound bridge that was tested.

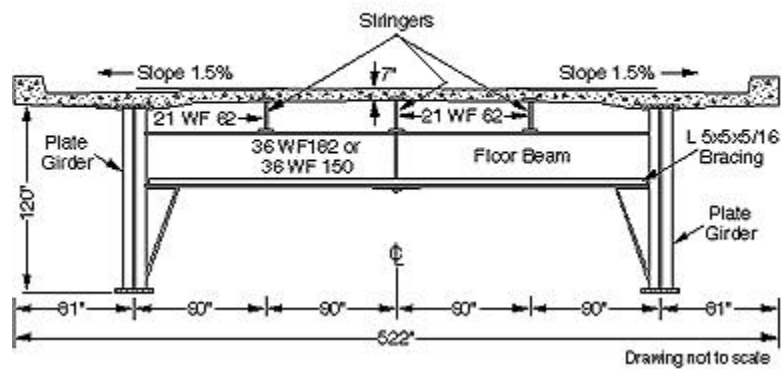


Fig. 5 Typical cross-section geometry of the bridge.

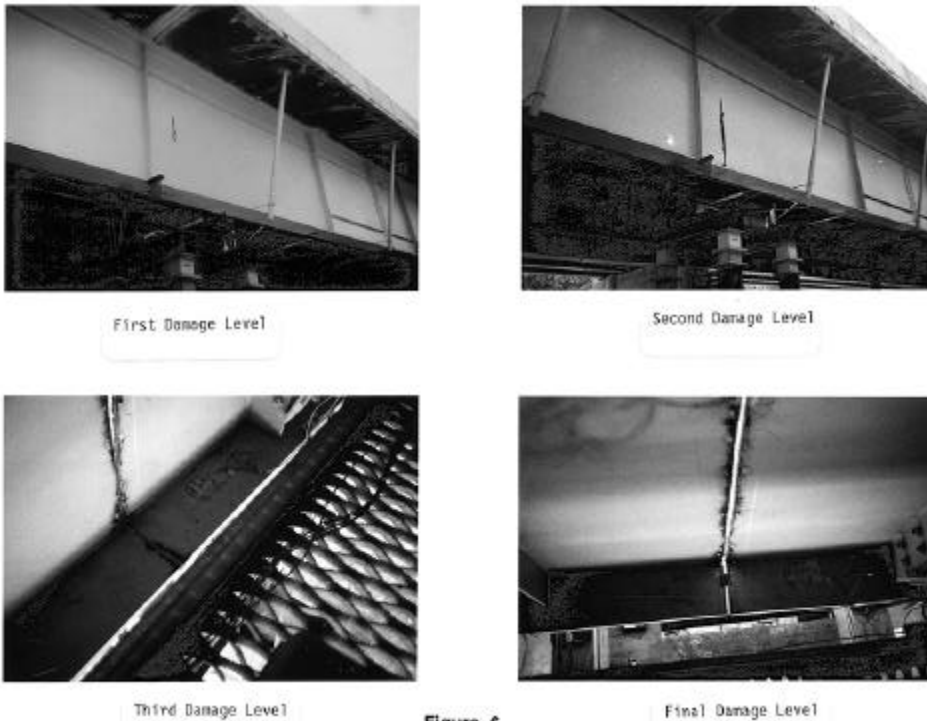


Fig. 6. Damage Introduced into the plate girder of the bridge.

peak. The algorithm that was used to perform this fit was developed specifically for this measurement system. The analytical function represents the sum of the real part of the Fourier spectra of a single degree-of-freedom system's response to a harmonic excitation plus a term to account for cross-talk between the drive signal and the measured response. This function has the form

$$F(\omega) = \text{Re} \left[\sum_{n=1}^{nm} \frac{A_n e^{i\omega t}}{\omega_n^2 - \omega^2 + i\omega^2 4\zeta^2 \omega_n^2} + A_0 e^{i\omega t} \right], \quad (4)$$

where $F(\omega)$ = the real portion of the measured displacement Fourier spectrum,

nm = the number of modes to be fit in a given frequency range,

ω_n = resonant frequency,

ζ = modal damping, and

A_n = the amplitude of the spectrum associated with ω_n .

A_0 is a background amplitude at ω , such as might occur with cross-talk between the harmonic input signal and the measured response signal. This cross-talk can result from radio frequency signals generated by the system powering the shaker. For the application reported herein a measurable amount of cross-talk could not be detected. A typical discrete spectrum that was obtained with the microwave interferometers operating in the homodyne detection mode is shown in Fig. 7 along with a function of the form of Eq. 4 that was fit to these data. This figure shows four distinct peaks indicating resonant frequencies. The less distinct peak at 3.5 Hz corresponds to a bending mode that has a node close to the microwave sensor location. Although the structure is symmetric, the connections of the plate girder to the piers are not symmetric. It is assumed that this small asymmetry is causing the response that is measured at this location. It should be noted that a typical complex receptance function could also be generated if the signal from the microwave sensor is normalized by the input force measurement.

The microwave sensors supplemented 26 conventional accelerometers that were also used to measure the vibration response of the bridge at locations shown in Fig. 8. Also shown in Fig. 8 are the location of the shaker, the damage location, and the locations of the microwave interferometers. These sensors measured the response of the bottom flange of the two main plate girders at the center of the mid-span of portion of the bridge that was tested. Experimental modal analyses using data from the accelerometers were performed before any damage had been introduced, and immediately after each stage of damage. In this context, experimental modal analysis refers to the procedure whereby a measured random excitation is applied to a structure and the structure's acceleration response is measured at discrete locations that are representative of the structure's motion. Both the excitation and the response time histories are then transformed into the frequency domain in the form of frequency response functions (FRF). Modal parameters (resonant frequencies, mode shapes, modal damping) can be determined by curve fitting analytical representations of the FRFs, defined in terms of these modal parameters, to the measured frequency domain data [6]. A rational-fraction polynomial global curve-fitting algorithm in a commercial modal-analysis software package was used to fit the analytical models to the measured FRF data and extract resonant frequencies, mode shapes and modal damping values. A detailed summary of all testing can be found in [1] and a discussion of the rational-fraction polynomial curve-fitting algorithm can be found in [7].

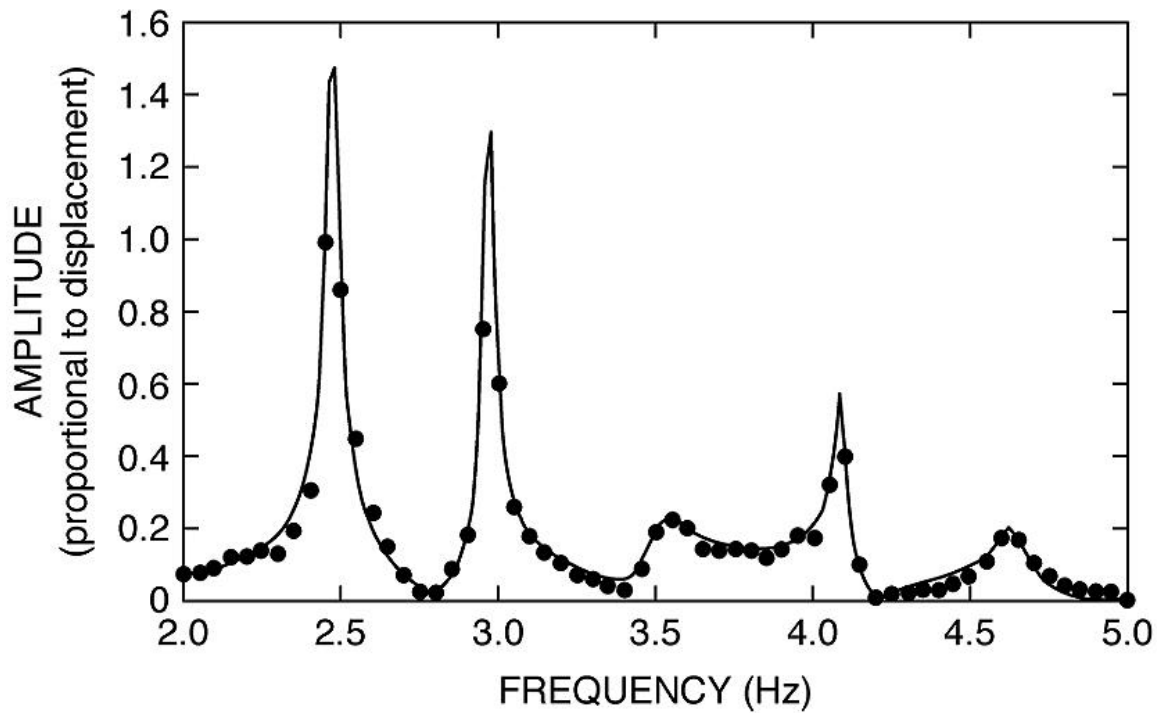


Fig. 7 A typical discrete spectrum measured with the microwave interferometer and the analytical spectrum that was fit to the measured data.

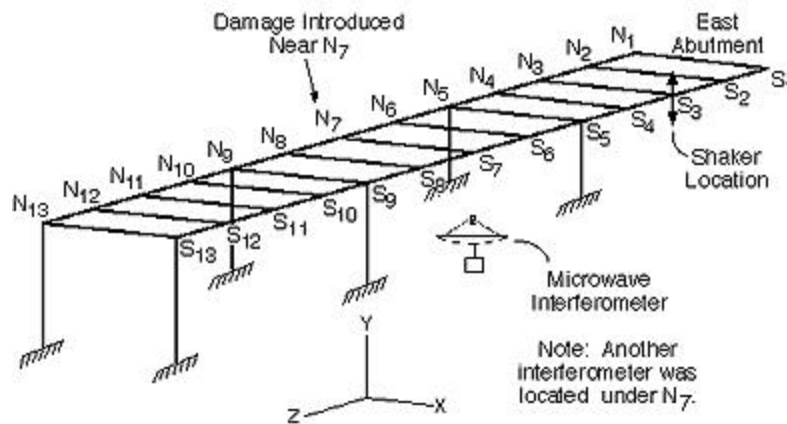


Fig. 8 Sensor locations for the bridge test.

V. Comparison with Conventional Accelerometer Measurements

The resonant frequencies and modal damping values identified from data obtained with the microwave interferometers are summarized in Table I. During the undamaged test and the test

performed after the first stage of damage, the curve-fitting routine was unable to distinguish modes 4 and 5, primarily as a result of the frequency resolution, but partially as a result of a lack of sophistication in the curve-fitting algorithm. It is clear from the accelerometer data presented below, that these modes are separated by approximately 0.1 Hz, which corresponds to only two data points with the 0.05 Hz resolution. Figure 9 compares the spectrum from the undamaged state with the spectrum corresponding to the final damage state. Distinct reductions in frequency associated with this most severe damage level are clearly visible in these spectra. Results from the experimental modal analyses based on data measured with conventional accelerometers are summarized in Table II. The frequency resolution of the FRFs generated from the accelerometer data was 0.0625 Hz. For the modes that could be identified with the microwave interferometer (modes 1-3, 6), the resonant frequencies measured with the interferometer agree well with corresponding values identified from data obtained with conventional accelerometers. All modes showed less than 2.2 percent difference in the identified resonant frequency. Damping values identified from data obtained with the microwave interferometers did not compare as consistently with values obtained from data measured with the accelerometers. This lack of agreement is attributed to the curve-fitting algorithm used with the microwave interferometer data and frequency resolution of these data, and does not reflect an inherent inability of the interferometer to measure the widths of the resonance peaks.

There is a small systematic increase in the resonant frequencies of most modes after the first and second cut. These increases range from 0.02 to 0.06 Hz. Similar increases are seen in both the accelerometer data and the data obtained with the microwave interferometers. The increases are believed to result from changes in the static loads on the bridge and inadvertent changes to the boundary conditions caused by demolition going on at the time of the testing.

VI. Concluding Comments

A microwave interferometer that overcomes the need for a mounted target was developed for remote, non-contact displacement vibration measurements. The sensors were coupled with homodyne detection hardware and software to measure the vibration response at two locations on a bridge structure. A comparison of the modal frequencies identified from microwave interferometer data to modal frequencies identified from data obtained with conventional accelerometers shows that the modal information being obtained with the interferometer is as accurate as that obtained with the conventional accelerometers. Complete mode shape data can be obtained if more interferometers are placed along the length of the beam at similar locations as the accelerometers. An obvious improvement to the analysis of data obtained from the interferometers would be to feed a calibrated analog displacement - time history from the interferometer directly into a data acquisition system. Then this signal could be digitized and analyzed with the more refined commercial modal analysis and digital signal processing software that is currently available.

These prototype interferometers were made from off-the-shelf electronic components that cost approximately \$1000 (U.S., 1997). Many engineering characteristics of these sensors have yet to be quantified. Further tests are needed using a moving surface whose motion is known to determine the effects of target surface reflectivity, the reflectivity from curved surfaces, the dispersion of the microwaves as a function of distance from the source, resolution limits, and upper frequency limitations. Further studies of angular motion of the target surface would also

TABLE I						
A Comparison of Resonance Frequencies and Modal Damping Identified from the Fits of Analytical Models to the Undamaged and Damaged Data Measured with the Microwave Interferometer						
	Mode 1	Mode 2	Mode 3	Mode 4	Mode 5	Mode 6
Test	Freq. (Hz)/ Damp. (%)	Freq. (Hz)/ Damp. (%)	Freq. (Hz)/ Damp. (%)	Freq. (Hz)/ Damp. (%)	Freq. (Hz)/ Damp. (%)	Freq. (Hz)/ Damp. (%)
Undamaged	2.48/ 0.91	2.98/ 1.61	3.53/ 3.19	4.12/ 0.79		4.67/ 0.65
After first cut	2.47/ 0.81	2.97/ 0.59	3.50/ 1.86	4.08/ 0.49		4.62/ 1.03
After second cut	2.50/ 1.59	3.00/ 0.67	3.57/ 0.56	3.98/ 1.01	4.14/ 0.72	4.70/ 0.79
After third cut	2.47/ 0.71	2.97/ 0.42	3.50/ 1.93	4.03/ 2.92	4.11/ 1.03	4.62/ 1.02
After final cut	2.25/ 3.56	2.84/ 0.70	3.45/ 2.39	3.96/ 1.96	4.12/ 2.61	4.55/ 0.93

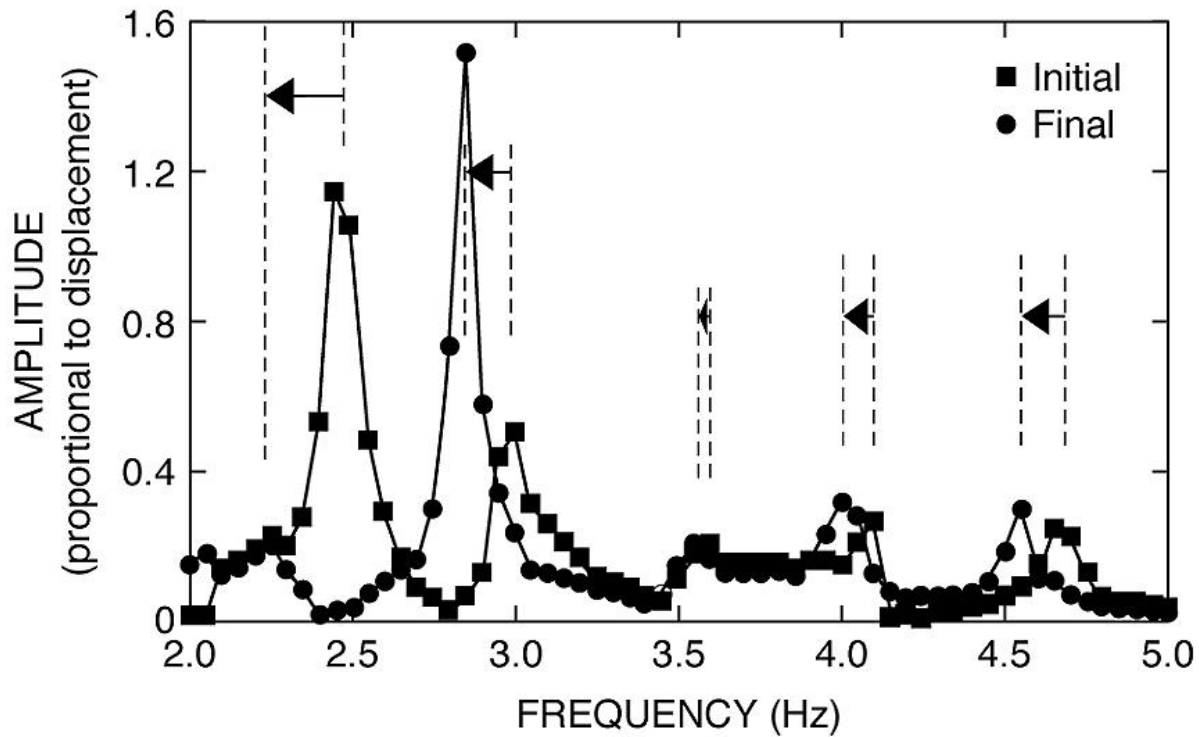


Fig. 9 Change in the spectrum that results from the final stage of damage.

TABLE II						
Resonant Frequencies and Modal damping Values Identified From Conventional Accelerometer Data Measured During Undamaged and Damaged Forced Vibration Tests						
	Mode 1	Mode 2	Mode 3	Mode 4	Mode 5	Mode 6
Test	Freq. (Hz)/ Damp. (%)	Freq. (Hz)/ Damp. (%)	Freq. (Hz)/ Damp. (%)	Freq. (Hz)/ Damp. (%)	Freq. (Hz)/ Damp. (%)	Freq. (Hz)/ Damp. (%)
undamaged	2.48/ 1.06	2.96/ 1.29	3.50/ 1.52	4.08/ 1.10	4.17/ 0.86	4.63/ 0.92
After first stage of damage	2.52/ 1.20	3.00/ 0.80	3.57/ 0.87	4.12/ 1.00	4.21/ 1.04	4.69/ 0.90
After second stage of damage	2.52/ 1.33	2.99/ 0.82	3.52/ 0.95	4.09/ 0.85	4.19/ 0.65	4.66/ 0.84
After third stage of damage	2.46/ 0.82	2.95/ 0.89	3.48/ 0.92	4.04/ 0.81	4.14/ 0.62	4.58/ 1.06
After final stage of damage	2.30/ 1.60	2.84/ 0.66	3.49/ 0.80	3.99/ 0.80	4.15/ 0.71	4.52/ 1.06

be beneficial. Finally, it is clear that to obtain accurate measurements with these sensors, the microwave source must be held in a fixed position during the data acquisition process or the motion of the sensor must be monitored.

VII. Acknowledgments

Funding for the development of this sensor was provided by the Federal Highway Administration through a project administered and jointly performed by New Mexico State University. The authors would like to acknowledge the cooperation and team work that was exhibited by all parties involved in these tests. This team includes engineers from Sandia National Laboratory, faculty, technicians and students from New Mexico State University; numerous people at the New Mexico State Highway and Transportation Department, and the staff of the Alliance for Transportation Research.

VIII. References

1. C. R. Farrar, et al., "Dynamic Characterization and Damage Detection in the I-40 Bridge over the Rio Grande," Los Alamos National Laboratory report LA-12767-MS, (June 1994) available at http://esaea-www.esa.lanl.gov/damage_id.
2. E. O. Doebelin, *Measurement Systems Application and Design*, 4th Ed., McGraw-Hill, New York, 1990.

3. T. G. Beckwith, R. D. Marangoni, and J. H. Lienhard, *Mechanical Measurements*, 5th Ed., Adisson-Wesley, Reading, MA, 1993.
4. J. Fraden, *AIP Handbook of Modern Sensors*, American Institute of Physics, New York, 1993.
5. R. L. Mayes and M. A. Nusser (1994) "The Interstate-40 Bridge Shaker Project," Sandia National Laboratory report SAND94-0228.
6. D. J. Ewins, *Modal Testing: Theory and Practice*, John Wiley, New York, 1985.
7. *Theoretical and Experimental Modal Analysis*, N. M. M. Maia and J. M. M. Silva, Edts., John Wiley and Sons, Inc., New York, 1997. pp 237 -248.